

Phonon Transmission by bcc Sandwich Layers in Fe/Co/Fe and Co/Fe/Co Systems

B. Bourahla, O. Nafa, A. Khater, R. Tigrine

A calculation of the coherent and ballistic phonon transport via thin nanojunctions between bcc lattices is presented. The model system A/B/A consists of a finite number of bcc (001) atomic layers of an element B sandwiched between two bcc semi-infinite crystal lattices of another element A oriented in the same (001) plane. It is applied to the Fe/Co/Fe nanojunction and to the inverse Co/Fe/Co nanojunction. The theoretical calculations of the ballistic phonon transmission via the nanojunction are carried out using the matching method. The possible experimental measurements of this ballistic transmission in comparison with theoretical results should be a useful probe for the determination of alloying force constants across the interface between two such elements. The full bcc dynamics of this system is under study.

1 Introduction

Current techniques make the fabrication of nanojunctions possible which consist of only few atomic layers sandwiched between semi infinite crystals. Such nanojunctions are of increasing importance in many technical applications, several examples are given by Tiusan et al. (2002), F. Haupt et al. (2009) and Oguz et al. (2009). The purpose of this communication is to present a calculation for the phonon ballistic transmission via a nanojunction of the A/B/A type where B is an ultra thin atomic layer sandwiched between two semi-infinite A crystals. In particular we apply the theoretical calculations to the case where A and B correspond alternatively to Fe and Co elements. The Fe/Cr/MgO/Fe nanojunction in the (001) plane and similar architectures are interesting candidates for the development of efficient magnetic tunnel junctions, see works of Matsumoto et al. (2009) and Mizuguchi et al. (2006). It is observed that the efficiency of these components is enhanced when an ultra thin layer of Cr is inserted at the interface of an epitaxial nanojunction Fe/MgO/Fe.

In Sect I, a description of the model is given and equations of motion are derived in a convenient form. In Section II, we present the numerical results for the coherent and ballistic phonon transmission coefficient as a function of the incident frequency.

2 Model Dynamics

Consider the system as indicated schematically in Figure 1 where the shaded area constitutes the effective nanojunction domain of B atoms. Although the crystalline structure is bcc, the model is treated as a simple cubic lattice with nearest neighbor interactions for both Fe and Co for the purpose of this calculation. This approximation simplifies our equations, and we shall justify it by making an analysis of the nearest and next nearest neighbor constants from available information on the elastic constants. The primary difficulty for the present work is how to derive appropriate force constants from the available elastic information for Fe and Co. Systematic ab-initio calculations of elastic constants, C_{11} , C_{12} , and C_{44} , for Fe and Co in the bcc structure have been carried out, in part to understand the phase stability and magnetic properties of Fe and Co nanostructures, presented by Guo (2000). To be able to extract information for the force constants from these results, we have exploited for the cubic lattices a method first proposed by Fuchs (1935-1936), and used by a number of authors to derive the ion-ion force constants for body centered cubic lattices, examples given by Jasmon (1954) and Bolef (1961), and simple cubic lattices presented by Khater et al. (2009).

Using this procedure we are able to derive the force constants between the nearest and next nearest neighbors for the bcc Fe and Co lattices, respectively as follows : $k_1(\text{Fe, Fe}) = 52.54 \text{ N/m}$, and $k_2(\text{Fe, Fe}) = 16.33 \text{ N/m}$, $k_1(\text{Co, Co}) = 70.92 \text{ N/m}$, and $k_2(\text{Co, Co}) = 8.74 \text{ N/m}$. Given the order of magnitude for the nearest and nearest neighbor force constants it seems reasonable to neglect the next nearest neighbor contributions for phonon propagation perpendicular to the (001) plane. The notation is hence simplified so that the nearest neighbor force constants on lattice A are denoted by k_A , and on lattice B by k_B . It is convenient next to define the following ratios:

$m = m_B/m_A$ for the masses, $r_d = k_{AB}/k_A$ where k_{AB} is the nearest neighbor force constant between an A and B sites at the nanojunction, and $r_B = k_B/k_A$. For the purpose of the calculation k_{AB} is considered as the arithmetic mean of the Fe and Co nearest neighbor force constants so that $k_{FeCo} = 61.04$ N/m.

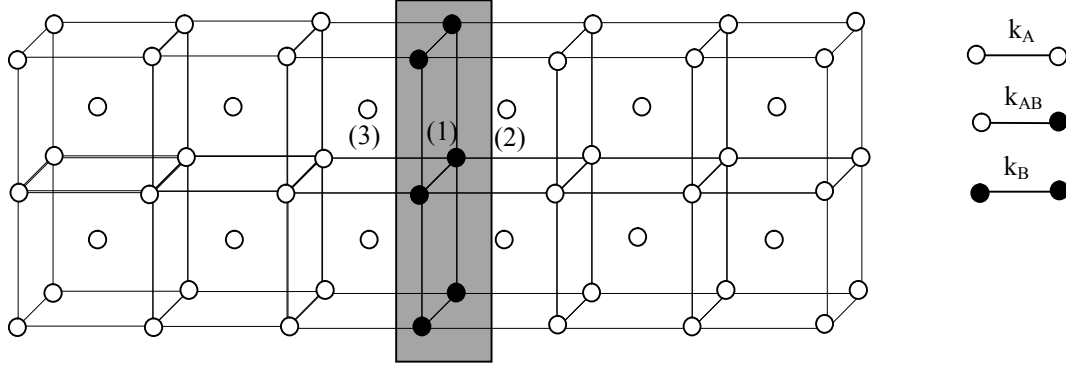


Figure 1. Schematic representation for a B layer sandwiched between two semi-infinite bcc A crystals. The shaded zone denotes the B layer of the nanojunction.

The dynamics of the perfect bcc system are described by the equations of motion of atomic sites l , which in the harmonic approximation, like given in Jzefel (1987), may be expressed as

$$\omega^2 m(l) u_\alpha(l) = - \sum_{l' \neq l} \sum_\beta k(l, l') d_\alpha d_\beta / d^2 [u_\beta(l) - u_\beta(l')] \quad (1)$$

$u_\alpha(l)$ is the corresponding vibration displacement vector for site l . The indices α, β denote Cartesian co-ordinates, and $m \equiv m(l)$ is the atomic mass of perfect site l . The atomic masses for Fe and Co are $m_{Fe} = 0.93 \cdot 10^{-24}$ kg and $m_{Co} = 0.98 \cdot 10^{-24}$ kg, respectively. The radius vector \mathbf{d} between sites at l and l' has Cartesian components d_α , and $d = |\mathbf{d}|$. The elastic force constants between any two given sites is denoted by $k(l, l')$, so that $k_1(l, l')$ and $k_2(l, l')$ are force constants between nearest and next nearest neighbor sites, respectively.

For sites l and l' distant from the inhomogeneous boundary to the left and right of the nanojunction in Figure 1, the equations of motion may be cast in the matrix form

$$[\Omega^2 I - D(e^{i\phi_x}, e^{i\phi_y}, e^{i\phi_z})] |u\rangle = 0 \quad (2)$$

$|u\rangle$ is the vector of vibration displacements along the principal axes in a unit cell. I denotes a unit matrix. $[\Omega^2 I - D(e^{i\phi_x}, e^{i\phi_y}, e^{i\phi_z})]$ is the bulk dynamics matrix, where $e^{i\phi_x}, e^{i\phi_y}$, and $e^{i\phi_z}$, are the Bloch phase factors along the principal axes, between neighboring sites in the unit cell. $\phi_\alpha = q_\alpha a$ is the normalized wave vector, and runs over the interval $[-\pi, +\pi]$ in the first BZ. $\Omega = \omega/\omega_0$ is a dimensionless frequency. Note that the characteristic frequency ω_0 is not the same for the Fe and Co lattices; ω_0 is $\sqrt{[k_1(Fe, Fe) / m_{Fe}]}$ for Fe, and $\sqrt{[k_1(Co, Co) / m_{Co}]}$, for Co, respectively. D is a (3×3) matrix.

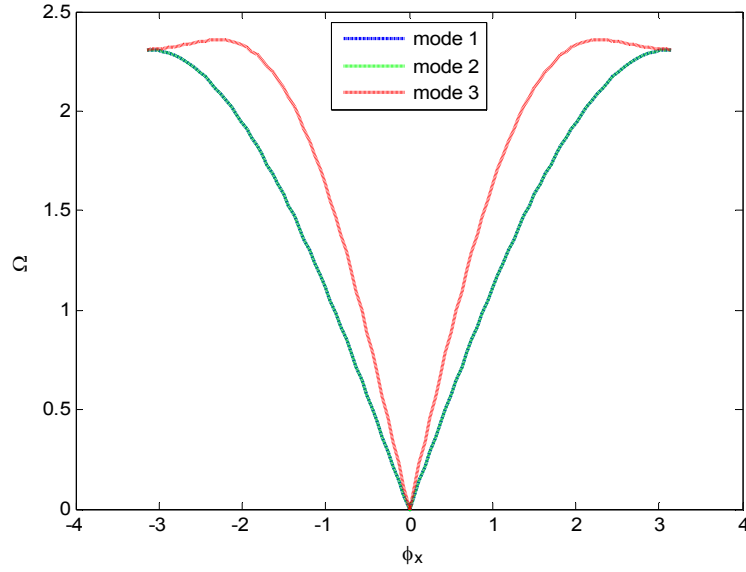


Figure 2. Phonon dispersion branches for the perfect bcc system along the x-direction

By diagonalizing the matrix of equation (2), one obtains the phonon dispersion branches. The branches along the x-direction are presented in Figure 2, in terms of the normalized frequency for each of the Fe and Co systems in the present approximation. The eigenmodes, labelled $i \in \{1, 2, 3\}$, are propagating in the following frequency interval: $\Omega = [\Omega_{\min} = 0.00, \Omega_{\max} = 2.35]$. These modes are acoustic, characterized by the limiting behaviour of their phonon branches, tending to zero frequency when the wave vector tends to zero. We note that two of the three modes are degenerate.

In order to render the problem tractable we need to decouple the dynamics of a representative and irreducible set of sites at the inhomogeneous boundary of the defect domain from the rest of the system. This irreducible set is comprised as in Figure 1, from the sites labeled (1), (2) and (3).

Consider a Hilbert space for the scattering and denote by $[|R\rangle, |T\rangle]$ the basis vector for the reflection and transmission coefficients in this space, and by $|U\rangle$ that for the displacements of a set of irreducible sites in the defect domain. The equations of motion for atoms of the scattering zone, coupled to the rest of the systems, may be written in terms of vector $[|U\rangle, |R\rangle, |T\rangle]$. The core vector $|U\rangle$, groups the atomic displacements for an irreducible set of sites on the boundary and a minimum representative subset of sites for the two matching regions.

Using the appropriate transformations connecting the displacement fields, and substituting these in equation (2), examples of application of ideas are given in Fellay et al. (1997), we obtain a square linear homogeneous system of equations in the form

$$[\Omega^2 I - D(e^{i\phi_x}, e^{i\phi_y}, e^{i\phi_z}, r, r_d)] [|U\rangle, |R\rangle, |T\rangle] = -|IH\rangle \quad (3)$$

In the defect domain $r_d = k_{AB}/k_A$ and $r = r_B$. The vector $-|IH\rangle$, mapped appropriately onto the basis vectors, regroups the inhomogeneous terms describing the incoming wave.

For non-trivial solutions for the components of the column vector $[|U\rangle, |R\rangle, |T\rangle]$, the determinant $[D(e^{i\phi_x}, e^{i\phi_y}, e^{i\phi_z}, r, r_d)]$ of the vibration dynamics matrix must vanish. This yields the energies of the vibration states on the inhomogeneous boundary.

The solution of equation (3) yields the displacements $|U\rangle$ of the irreducible set of atomic sites for the defect domain, as well as the components R_{ij} and T_{ij} .

The scattering behavior is usually described in terms of the scattering matrix, which elements are given by the relative reflection and transmission probabilities r_{ij} and t_{ij} at the scattering frequency Ω . These are given by

$$r_{ij} = (V_{gi} / V_{gi}) |R_{ij}|^2 \quad \text{and} \quad t_{ij} = (V_{gj} / V_{gi}) |T_{ij}|^2 \quad (4)$$

V_{gi} is the group velocity.

The scattering of the phonons at the sandwich layers domain is studied with reference to incident phonons of the perfect wave-guide, which is split at the nanojunction into its transmitted and reflected parts.

3 Numerical Applications and Conclusion

The numerical analysis is carried out for the two types of nanojunctions Fe/Co/Fe and Co/Fe/Co, where the number of the irreducible atomic layers for a nanojunction is composed of three atomic layers. Since the masses of Fe and Co are very comparable, $m_{Fe} \sim m_{Co}$, the first system Fe/Co/Fe corresponds effectively to a case of hardening of elastic constants on the nanojunction, for which $m = 1.05$, $r_B = 1.35$, and $r_d = 1.16$, whereas the second system Co/Fe/Co corresponds to a case of softening of elastic constants on the nanojunction, for which $m = 0.95$, $r_B = 0.74$, $r_d = 0.86$.

The transmission and the reflection spectra verify the unitarity condition $s = t_i + r_i = 1$ per the i th mode at all propagating frequencies, and this is systematically used as a check on the numerical calculations. In Figures 3a and 3b, the transmission spectra are presented as a function of the dimensionless frequency.

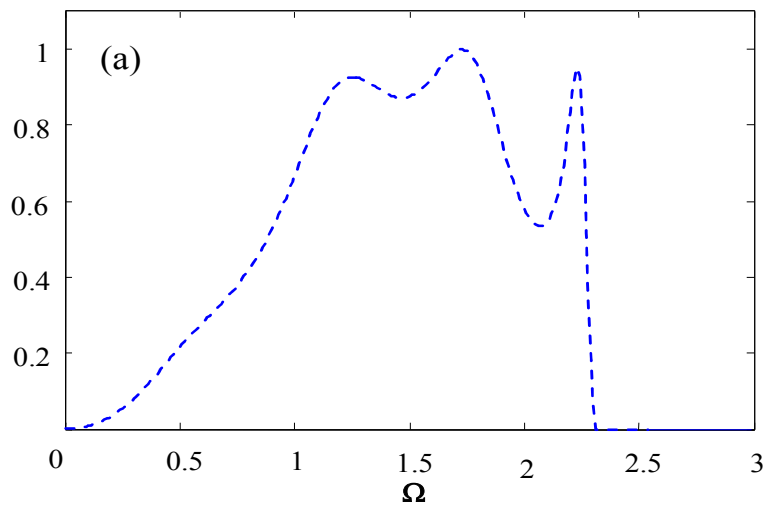


Figure 3a. Coherent phonon transmission via the Fe/Co/Fe nanojunction as a function of the dimensionless frequency, for $m = 1.05$, $r_B = 1.35$, $r_d = 1.16$.

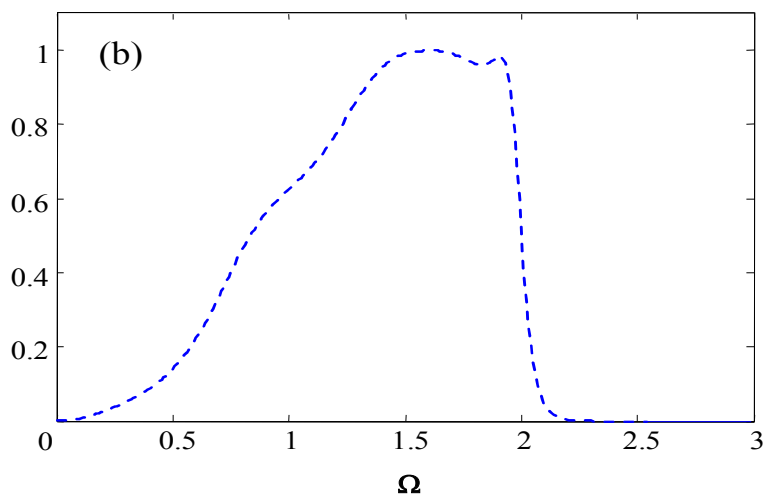


Figure 3b. Coherent phonon transmission via the nanojunction Co/Fe/Co as a function of the dimensionless frequency, for $m = 0.95$, $r_B = 0.74$, $r_d = 0.86$.

The observed overall transmission spectra, in Figures 3a and 3b summing over the propagating modes, are comparable but not identical. In both cases they are inside a rectangular box histogram with a base line bounded by $0 \leq \Omega \leq \pi$, and by the closed interval $[0, 1]$ that corresponds to a unity height for the transmission of the phonons, for both ideal cases of the Fe or Co waveguide systems.

The transmission spectra are attributed to the coupling of the propagating incident phonon with a localized vibration modes induced by the sandwich layer in the nanojunction in each case. At small frequencies the two systems present quite comparable properties with monotonically decreasing transmission. Note, however, that for the hardening case we observe in Figure 3a three peaks at the frequencies $\Omega = 1.25, 1.75$ and 2.25 , whereas for the softening case there is a broad band as in Figure 3b. The peaks in Figure 3a, in comparison with experimental data which is unavailable at present, may eventually provide more precise information as regards the value of the nearest neighbor alloying type force constant $k_1(\text{Fe, Co})$ between the two elements at the nanojunction.

In conclusion, we have presented a model calculation for the study of phonon scattering and transmission via a nanojunction. This analysis enables one to address questions regarding the mechanical properties of the substitution layers in the perfect lattice.

References

- Tiusan, C.; Hehn, M.; Ounadjela, K.: Magnetic-roughness-induced magnetostatic interactions in magnetic tunnel junctions. *Eur. Phys. J. B* 26, (2002), 431-434.
- Haupt, F.; Novotny, T.; Belzig, W.: Phonon-assisted current noise in molecular junctions. *Phys. Rev. Lett.* 103, (2009), 136601-136613.
- Oguz, K.; Coey, J. M. D.: Room-temperature magnetoresistance in CoFeB/STO/CoFeB magnetic tunnel junctions. *J. Mag. Mag. Mat.* 321, (2009), 1009-1011.
- Matsumoto, R.; Fukushima, A.; Yakushiji, K.; Nishioka, S.; Nagahama, T.; Katayama, T.; Suzuki, Y.; Ando, K.; Yuasa, S.: Spin-dependent tunneling in epitaxial Fe/Cr/MgO/Fe magnetic tunnel junctions with an ultrathin Cr(001) spacer layer. *Phys. Rev. B* 79, (2009), 174436-174443.
- Mizuguchi, M.; Suzuki, Y.; Nagahama, T.; Yuasa, S.: Scanning tunnelling microscopy observations of single-crystal FeMgO/Fe magnetic tunnel junctions. *J. Appl. Phys.* 99, (2006) 08A907-08A909.
- Guo, G.Y.; Wang, H. H.: Gradient-Corrected Density Functional Calculation of Elastic Constants of Fe, Co and Ni in bcc, fcc and hcp Structures. *Chin. J. Phys.* 38, (2000), 949-961.
- Fuchs, K.: A quantum mechanical investigation of the cohesive forces of metallic copper. *Proc. Roy. Soc. London A* 151, (1935), 585-602.; Fuchs, K.: Quantum-mechanical calculation of the elastic constants of monovalent metals. *Proc. Roy. Soc. London A* 153, (1936), 622-639.
- Bolef, D.I.: Elastic Constants of Single Crystals of the bcc Transition Elements V, Nb, and Ta. *J. Appl. Phys.* 32, (1961), 100-105.
- Jaswon, M. A.: *The Theory of Cohesion*. Interscience Publishers, Inc., New York (1954).
- Khater, A.; Tigrine, R.; Bourahla, B.: Polonium bulk and surface vibrational dynamics. *Phys. Status Solidi (b)*: 246, (2009), 1614-1617.
- Szeftel, J.; Khater, A.: Calculation of surface phonons and resonances: the matching procedure revisited: I. *J. Phys. C: Solid St. Phys.* 20, (1987), 4725-4736.
- Fellay, A.; Gagel, F.; Maschke, K.; Virlovvet A.; Khater, A.: Scattering of vibrational waves in perturbed quasi-one-dimensional multichannel waveguides. *Phys. Rev. B* 55, (1997), 1707-1717.

B. Bourahla^{1,2}, O. Nafa¹, A. Khater², R. Tigrine^{1,2}

Address: ⁽¹⁾Laboratoire de Physique et Chimie Quantique, Université M. Mammeri, 15000 Tizi-Ouzou, Algérie

⁽²⁾Laboratoire de Physique de l'Etat Condensé UMR 6087, Université du Maine, 72085 Le Mans, France

email: bourahla_boualem@yahoo.fr, ouahibanafa@yahoo.fr, antoine.khater@uni-lemans.fr, tigriner@yahoo.fr